

First-principles study of exchange stiffness constant of half-metallic Heusler alloys Co_2MnZ ($Z = \text{Si}, \text{Al}$) at finite temperatures: Spin fluctuation-induced effective half metallicity

Shogo Yamashita* and Akimasa Sakuma

Department of Applied Physics, Tohoku University, Sendai 980-8579, Japan

Mikihiko Oogane

Department of Applied Physics, Tohoku University, Sendai 980-8579, Japan

(Dated: September 24, 2024)

We performed first-principles calculations at finite temperatures to investigate the temperature dependence of the magnetic properties, such as exchange stiffness constants and Curie temperatures, of Co_2MnZ ($Z = \text{Si}, \text{Al}$) assuming $L2_1$ and $B2$ structures. In $L2_1$ structures, we confirmed a relatively high Curie temperature for Co_2MnAl , compatible with that of Co_2MnSi ; however, its exchange stiffness constant and single site magnetic excitation energy at zero temperature are much smaller than those of Co_2MnSi . This might indicate that the Curie temperature of itinerant magnets cannot be determined by the exchange interaction at zero temperature. We also investigated the temperature dependence of the exchange stiffness constants of both alloys, and we found robustness in the temperature dependence of the exchange stiffness constant for Co_2MnAl , assuming an $L2_1$ structure. This might lead to a high Curie temperature, contrary to the small exchange stiffness constant. Finally, we examined the temperature dependence of the electronic structure to investigate the origin of the behavior of the exchange stiffness constant at finite temperatures. We confirmed that the spin polarization at chemical potential effectively increases with an increasing temperature due to the altered electronic structure induced by the spin disorder. This might contribute to the robustness of the exchange stiffness constant at finite temperatures. Our results might indicate that renormalization of the electronic structure due to spin disorder at finite temperature influences the exchange interactions of Co_2MnAl .

I. INTRODUCTION

Half-metallic Co-based full-Heusler alloys Co_2MnZ ($Z = \text{Si}, \text{Al}$) are technologically important materials in the field of spintronics due to their high Curie temperatures, large magnetization, and theoretically predicted high spin polarization, approximately 100% at the Fermi level[1–3]. A notable application example of $\text{Co}_2\text{MnSi}(\text{Al})$ is that for spintronics devices based on magnetic tunnel junctions (MTJ), which exhibit a large tunnel magnetic resistance (TMR) effect. In fact, experimentally, a large TMR ratio has been achieved in MTJs where $\text{Co}_2\text{MnSi}(\text{Al})$ is used for the electrodes, not only at low temperatures but also at room temperatures and half-metallic characters have been confirmed[4–8]. The TMR ratio usually decreases with an increasing temperature, and it is mainly considered that thermal spin fluctuations at the ferromagnet and barrier interface cause this reduction[9]. In addition, it has also been theoretically confirmed that the exchange interactions at the $\text{Co}_2\text{MnSi}(\text{Al})/\text{MgO}$ interface become weak compared with those in the of bulk, in particular, the exchange interaction at Co sites[10], and the thermal spin fluctuations (non-collinear spin structure) at the $\text{Co}_2\text{MnSi}/\text{MgO}$ interface reduce the TMR ratio[11]. Therefore, to improve the TMR ratio at finite-temperatures, it is important to enhance the exchange stiffness constant A (or spin stiffness constant D) at the interface to suppress thermal spin fluctuations. The exchange stiffness constant is one of the indicators that show the strength of the exchange interactions in magnetic materials, namely, the robustness of the magnetic moments against thermal spin fluctuations. It is also an important parameter for micromagnetic

simulations to calculate the dynamics of magnetization, as well as the magnetic anisotropy constant and Gilbert damping constant.

Apart from the interfaces, the temperature dependence of exchange stiffness constants (or thermal spin fluctuation) in $\text{Co}_2\text{MnSi}(\text{Al})$ compounds may also contribute to a secondary reduction in the TMR ratio at finite temperatures. The exchange stiffness constants of $\text{Co}_2\text{MnSi}(\text{Al})$ compounds have been measured in several experiments[12–16]. Among them, Kubota et al.[15] reported a significantly smaller (five times) exchange stiffness constant of Co_2MnAl compared with that of Co_2MnSi , which were measured by them or Hamrle et al.[14] at room temperature with Brillouin light scattering spectroscopy. Meanwhile, the experimental results of the spin stiffness constants measured by Umetsu et al.[16] from the temperature dependence of magnetization at low temperature are not so different between Co_2MnSi and Co_2MnAl . Therefore, to explain this experimental difference, a comprehensive theoretical understanding of the exchange stiffness constants, not only at low-temperatures but also at room temperature or the entire temperature range, may be required.

Theoretically, the temperature dependence of the exchange stiffness constants is described by the magnon magnon scattering theory based on the localized Heisenberg Hamiltonian as proposed by Dyson[17]. However, nowadays, $3d$ electrons in the metallic magnetic systems are regarded as itinerant electrons. They have contradictory dual properties including hybridization effects with other orbitals and large local magnetic moments, which are non-integer values[21, 22]. In fact, it has been theoretically shown that the gaps in the minority spin states of $\text{Co}_2\text{MnSi}(\text{Al})$ originate from the hybridization of d orbitals of Co-Co atoms, and the hybridization of Mn-Co also plays an important role to determine its electronic

* shogo.yamashita.q1@dc.tohoku.ac.jp

structure[2, 3]. Moreover, it has been shown that the magnetic moments of Co atoms are less localized compared with those of Mn atoms using x-ray absorption and x-ray magnetic circular dichroism techniques[18–20]. In this sense, $\text{Co}_2\text{MnSi}(\text{Al})$ compounds may be typical examples where $3d$ electrons have dual itinerant and localized properties. Therefore, the localized spin models, such as the Heisenberg model, which are appropriate for magnetic insulators or $4f$ electron systems, may not be appropriate approaches for these alloys to capture magnetic properties, not only at zero temperature but also at finite temperatures. Based on the above mentioned concept, in previous works[23, 24], we established a theory to describe the temperature dependence of the exchange stiffness constants based on the functional integral method for itinerant electron systems[21, 25–30], combined with the disordered local moment (DLM) picture based on the coherent potential approximation (CPA). The DLM-CPA theory was originally proposed in the first-principles calculation based on the Korringa-Kohn-Rostoker method[31–37], and we reformulated it in the tight-binding linear muffin-tin orbital (TB-LMTO) method in our previous works[23, 24, 38–42]. Therefore, by using our developed theory, we can investigate the exchange stiffness constant of the Heusler alloys at finite temperatures based on the electronic structures, which include both itinerant and localized characters of d electrons. In this study we investigated the exchange stiffness constants of $\text{Co}_2\text{MnSi}(\text{Al})$ with B2 or L2_1 structures, not only at zero temperature but also at finite temperatures, and found unique behavior for Co_2MnAl with L2_1 structure at finite temperatures. We also examined the effect of spin fluctuation (spin disorder) at finite-temperatures for the electronic structures and exchange interactions of $\text{Co}_2\text{MnSi}(\text{Al})$ and discussed the relationship between them.

II. THEORETICAL METHOD

We use the TB-LMTO method[43–47] combined with the atomic sphere approximation (ASA) to construct a first-principles functional integral theory. The functional integral to evaluate the partition function Z and free energy F are given as follows:

$$Z = \int \left(\prod_i d\mathbf{e}_i \right) \exp(-\Omega(T, \{\mathbf{e}\})/k_B T), \quad (1)$$

$$F = \langle \Omega(T, \{\mathbf{e}\}) \rangle_{\omega(T, \{\mathbf{e}\})} + k_B T \langle \ln \omega(T, \{\mathbf{e}\}) \rangle_{\omega(T, \{\mathbf{e}\})} + \mu N_e, \quad (2)$$

where

$$\langle \cdots \rangle_{\omega(T, \{\mathbf{e}\})} = \int \left(\prod_i d\mathbf{e}_i \right) \omega(T, \{\mathbf{e}\}) \cdots. \quad (3)$$

Here, μ and N_e are chemical potential and electron number of the system, respectively. The thermodynamic potential Ω can be decomposed as follows:

$$\Omega = \Omega_{\text{SP}} + \Omega_{\text{DC}}, \quad (4)$$

where Ω_{SP} and Ω_{DC} are the thermodynamic potentials of the single-particle and double counting part. The thermodynamic potentials are evaluated within an adiabatic approximation because of low energy scale (slow motion) of spin fluctuations compared to the energy scale of hopping of electrons. Here, to simplify the theory, we are based on the magnetic force theorem to evaluate the magnetic excitation energy with respect to its directions keeping its lengths. This means that only spin-transverse fluctuations are included and the longitudinal fluctuations are ignored in our formalism. In addition, we use the local spin density approximation (LSDA) as the exchange correlation potential to calculate the thermodynamic potential of the single-particle part. Therefore, the distribution of the spin configuration $\omega(T, \{\mathbf{e}\})$ at temperature T is given as follows:

$$\omega(T, \{\mathbf{e}\}) \sim \exp(-\Omega_{\text{SP}}(T, \{\mathbf{e}\})/k_B T) / Z_{\text{SP}}, \quad (5)$$

$$\Omega_{\text{SP}}(T, \{\mathbf{e}\}) = \frac{1}{\pi} \int d\epsilon f(\epsilon, T, \mu) \int_{-\infty}^{\epsilon} dE \text{ImTr } G(z; \{\mathbf{e}\}), \quad (6)$$

where $z = E + i\delta$. δ is fixed to 2 mRyd. Owing to the force theorem, we dropped the double counting term to evaluate the spin configuration $\omega(T, \{\mathbf{e}\})$. Here, the Green function of the system $G(z; \{\mathbf{e}\})$ is introduced as follows:

$$G_{ij}(z; \{\mathbf{e}\}) = (z - H_{\text{TB-LMTO}}(\{\mathbf{e}\}))_{ij}^{-1} \\ = \tilde{\lambda}_i^\alpha(z; \mathbf{e}_i) \delta_{ij} + \tilde{\mu}_i^\alpha(z; \mathbf{e}_i) g_{ij}^\alpha(z; \{\mathbf{e}\}) (\tilde{\mu}_j^\alpha(z; \mathbf{e}_j))^\dagger, \quad (7)$$

$$H_{\text{TB-LMTO}}(\{\mathbf{e}\}) \\ = \tilde{C}(\{\mathbf{e}\}) + \tilde{\Delta}^{\frac{1}{2}}(\{\mathbf{e}\}) S (1 - \tilde{\gamma}(\{\mathbf{e}\}) S)^{-1} \tilde{\Delta}^{\frac{1}{2}}(\{\mathbf{e}\}), \quad (8)$$

where $\tilde{A}(\{\mathbf{e}\})$ is given as $U^\dagger(\{\mathbf{e}\}) A U(\{\mathbf{e}\})$ and C, γ, Δ are potential parameters in the TB-LMTO method. S is a bare structure constant. λ_i^α and μ_i^α are given as follows:

$$\lambda_i^\alpha(z) = \Delta_i^{-\frac{1}{2}} (1 + (\gamma_i - \alpha) P_i^\gamma(z)) \Delta_i^{-\frac{1}{2}}, \quad (9)$$

$$\mu_i^\alpha(z) = \Delta_i^{-\frac{1}{2}} (P_i^\gamma(z))^{-1} P_i^\alpha(z), \quad (10)$$

$$(\mu_i^\alpha(z))^\dagger = P_i^\alpha(z) (P_i^\gamma(z))^{-1} \Delta_i^{-\frac{1}{2}}, \quad (11)$$

$$P_i^\gamma(z) = \Delta_i^{-\frac{1}{2}} (z - C_i) \Delta_i^{-\frac{1}{2}}, \quad (12)$$

$$P_i^\alpha(z) = P_i^\gamma(z) [1 - (\alpha - \gamma_i) P_i^\gamma(z)]^{-1}, \quad (13)$$

$$g_{ij}^\alpha(z; \{\mathbf{e}\}) = [(\tilde{P}^\alpha(z; \{\mathbf{e}\}) - S^\alpha)^{-1}]_{ij}, \quad (14)$$

where α is a site-independent matrix of maximum localized representation, which is summarized in several references.

Here, S^α is given as $S(1 - \alpha S)^{-1}$. In practice, we cannot treat various patterns of spin configuration $\{\mathbf{e}\}$ in the functional integral. Therefore, we adopt the CPA and single-site approximation to determine $\omega(T, \{\mathbf{e}\})$. Here, we decompose $\Omega_{\text{SP}}(T, \{\mathbf{e}\})$ and $\omega(T, \{\mathbf{e}\})$ as follows:

$$\Omega_{\text{SP}}(T, \{\mathbf{e}\}) = \Omega_{\text{SP}}^0 + \sum_i \Delta\Omega_{\text{SP}}(T, \mathbf{e}_i), \quad (15)$$

$$\omega(T, \{\mathbf{e}\}) = \prod_i \omega_i(T, \mathbf{e}_i). \quad (16)$$

The first term in Eq. (15) is independent on spin configuration. Therefore, the decomposed distribution of spin configuration $\omega_i(T, \mathbf{e}_i)$ is calculated by using only the second term in Eq. (15) as follows:

$$\begin{aligned} \omega_i(T, \mathbf{e}_i) &= \exp(-\Delta\Omega_{\text{SP}}(T, \mathbf{e}_i)/k_B T) / \int d\mathbf{e}_i \exp(-\Delta\Omega_{\text{SP}}(T, \mathbf{e}_i)/k_B T). \end{aligned} \quad (17)$$

Here, we can obtain $\Delta\Omega_{\text{SP}}(T, \mathbf{e}_i)$ from the following equations:

$$\begin{aligned} \Delta\Omega_{\text{SP}}(T, \mathbf{e}_i) &= -\frac{1}{\pi} \int d\epsilon f(\epsilon, T, \mu) \text{Im}[\text{Tr}_{L\sigma} \log \lambda_i^\alpha(z) \\ &\quad - \text{Tr}_{L\sigma} \log(1 + \Delta P_i(z; \mathbf{e}_i) \bar{g}_{ii}^\alpha(z))], \end{aligned} \quad (18)$$

$$\Delta P_i(z; \mathbf{e}_i) = \bar{P}_i^\alpha(z; \mathbf{e}_i) - \bar{P}_i(z), \quad (19)$$

$$\bar{g}^\alpha(z) = (\bar{P}(z) - S^\alpha)^{-1}, \quad (20)$$

where $\bar{g}^\alpha(z)$ and $\bar{P}(z)$ are the coherent Green function and coherent potential function. Here, we used the fact that $\text{Tr}_{L\sigma} \ln \tilde{\lambda}_i^\alpha(z; \mathbf{e}_i) = \text{Tr}_{L\sigma} \ln \lambda_i^\alpha(z)$, and thus the first term of Eq. (18) becomes independent of the spin configuration. $\bar{g}^\alpha(z)$ and $\bar{P}(z)$ are obtained from the following CPA condition together with Eq. (19) and (20) in a self-consistent manner:

$$\int d\mathbf{e}_i \omega_i(T, \mathbf{e}_i) [1 + \Delta P_i(z; \mathbf{e}_i) \bar{g}_{ii}^\alpha(z)]^{-1} \Delta P_i(z; \mathbf{e}_i) = 0. \quad (21)$$

Once we obtain the decomposed distribution of spin configuration $\omega_i(T, \mathbf{e}_i)$, we can calculate the thermodynamic potential of the single particle part as follows:

$$\langle \Omega_{\text{SP}} \rangle_{\{\omega_i(T, \mathbf{e}_i)\}} = \sum_i \int d\mathbf{e}_i \omega_i(T, \mathbf{e}_i) \Omega_{\text{SP}}(T, \mathbf{e}_i), \quad (22)$$

$$\begin{aligned} \Omega_{\text{SP}}(T, \mathbf{e}_i) &= -\frac{1}{\pi} \text{Im} \text{Tr}_{L\sigma} \int_{-\infty}^{\infty} d\epsilon \epsilon f(\epsilon, T, \mu) G_{ii}(\epsilon + i\delta, \mathbf{e}_i) \\ &\quad - \frac{k_B T}{\pi} \text{Im} \text{Tr}_{L\sigma} \int_{-\infty}^{\infty} d\epsilon G_{ii}(\epsilon + i\delta, \mathbf{e}_i) \\ &\quad \times (f(\epsilon, T, \mu) \log f(\epsilon, T, \mu) + (1 - f(\epsilon, T, \mu)) \log(1 - f(\epsilon, T, \mu))) \end{aligned} \quad (23)$$

$$G_{ii}(z, \mathbf{e}_i)$$

$$= \tilde{\lambda}_i^\alpha(z, \mathbf{e}_i) + \tilde{\mu}_i^\alpha(z, \mathbf{e}_i) \bar{g}_{ii}^\alpha(z) (1 + \Delta P_i(z, \mathbf{e}_i) \bar{g}_{ii}^\alpha(z))^{-1} (\tilde{\mu}_i^\alpha(z, \mathbf{e}_i))^\dagger. \quad (24)$$

Hereafter, we introduce an external force to express the spin-spiral magnetic structures labeled by \vec{q} in the magnetically disordered environment at finite temperatures. For this purpose, we use the generalized Bloch's theorem[48–51] and transform the bare structure constant as follows[23, 52, 53]:

$$\tilde{S}_{ij}(\vec{k}, \vec{q}) = U_i \begin{pmatrix} S_{ij}(\vec{k} - \frac{\vec{q}}{2}) & 0 \\ 0 & S_{ij}(\vec{k} + \frac{\vec{q}}{2}) \end{pmatrix} U_j^\dagger, \quad (25)$$

where i and j stand for sites of the sub-lattice in each unit cell, and we redefine U at site i as follows:

$$U_i = \frac{1}{\sqrt{2}} \begin{pmatrix} e^{i(\frac{\vec{q}}{2} \cdot \vec{r}_i)} & e^{-i(\frac{\vec{q}}{2} \cdot \vec{r}_i)} \\ -e^{i(\frac{\vec{q}}{2} \cdot \vec{r}_i)} & e^{-i(\frac{\vec{q}}{2} \cdot \vec{r}_i)} \end{pmatrix}, \quad (26)$$

where \vec{r}_i denotes sub-lattice positions in each unit cell. Therefore, in the spin-spiral magnetic state, the coherent Green function in Eq. (24) is replaced as follows:

$$\bar{g}_{ii}^\alpha(z, \vec{q}) = \frac{1}{N} \sum_{\vec{k}} \left[(\bar{P}(z) - S^\alpha(\vec{k}, \vec{q}))^{-1} \right]_{ii}, \quad (27)$$

where N is a number of k -points in the Brillouin zone. By using Eqs. (22), (23), (24), and (27), we calculate the free energy difference at temperature T as follows:

$$\Delta F(\vec{q}, T) \sim \langle \Omega_{\text{SP}}(\vec{q}) \rangle_{\{\omega_i(T, \mathbf{e}_i)\}} - \langle \Omega_{\text{SP}}(\vec{q} = 0) \rangle_{\{\omega_i(T, \mathbf{e}_i)\}}. \quad (28)$$

It can be noted that $\omega_i(T, \mathbf{e}_i)$ has \vec{q} dependence; however, we focus on the vicinity of $\vec{q} = 0$ to calculate the exchange stiffness constant. Therefore, we neglect the \vec{q} dependence of $\omega_i(T, \mathbf{e}_i)$. Here, we use the magnetic force theorem again and do not include the double counting term to calculate the free energy difference. Once we obtain the free energy difference $\Delta F(\vec{q}, T)$, we can calculate the exchange stiffness constant at finite temperatures as follows:

$$A_\eta(T) = \frac{1}{2V} \frac{d^2 \Delta F(\vec{q}, T)}{dq_\eta^2} \Big|_{q_\eta=0}. \quad (29)$$

In this study, η is fixed to the z -direction. In particular, the spin stiffness constant at zero temperature D is given as follows:

$$D_\eta = \frac{4V}{M} A_\eta(0), \quad (30)$$

where M and V are the magnetization at zero temperature and a volume of the unit cell, respectively. The details of the DLM-CPA method in the TB-LMTO method are also summarized in references[23, 24, 38–42]. $20 \times 20 \times 20$ k -points are used for the calculations of exchange stiffness constants, and $30 \times 30 \times 30$ k -points are used for the calculation of the spin polarization ratio. The structure constants are expanded up to d -orbitals. The lattice constants are set to 5.654 and 5.756 for Co_2MnSi and Co_2MnAl with $L2_1$ structure, respectively. For $B2$ structure, half values of them are adopted. The spin-orbit coupling is ignored in this study.

III. RESULTS

A. Zero-temperature properties

We summarize calculated the magnetic properties of Co_2MnSi and Co_2MnAl at zero temperature in Table I. From this table, we can observe that the exchange stiffness constant of Co_2MnAl with $L2_1$ structure is almost half compared with that of Co_2MnSi with $L2_1$ structure. However, if we focus on the results for B2 structures, the exchange stiffness constants of Co_2MnSi and Co_2MnAl do not differ significantly from each other. The calculated magnetic moments are also summarized in Table I. The total magnetic moments of Co_2MnSi and Co_2MnAl with $L2_1$ structure are close to $5 \mu_B$ and $4 \mu_B$, respectively. Our calculated magnetic moments are in good agreement with those in previous studies[2, 3, 54, 55] with the LSDA.

To investigate the reason why the exchange stiffness constant of Co_2MnAl with $L2_1$ structure is much smaller than that of Co_2MnSi , we examined the electron filling dependence of the exchange stiffness constant for both alloys. In addition, we also examined the on-site magnetic excitation energy of the infinitesimal spin-rotation J_o at site o with the so called Lichtenstein-Katsnelson-Antropov-Gubanov (LKAG) formula[56, 57] as follows:

$$J_o = -\frac{1}{4\pi} \text{Im} \int_{-\infty}^{E_F} d\epsilon \text{Tr}_L \{ \Delta P_o^\gamma(\epsilon) (g_{oo\uparrow\uparrow}^\gamma(\epsilon) - g_{oo\downarrow\downarrow}^\gamma(\epsilon)) + \Delta P_o^\gamma(\epsilon) g_{oo\uparrow\uparrow}^\gamma(\epsilon) \Delta P_o^\gamma(\epsilon) g_{oo\downarrow\downarrow}^\gamma(\epsilon) \}, \quad (31)$$

where we defined $\Delta P_o^\gamma(\epsilon) = P_o^{\gamma\uparrow}(\epsilon) - P_o^{\gamma\downarrow}(\epsilon)$. We show the calculated electron filling dependence of A and J_o for Co_2MnSi and Co_2MnAl with $L2_1$ structures in Fig. 1. Here, we assumed the rigid band model. We changed the total electron number in the unit cell to shift the Fermi level and calculated A and J_o for each Fermi level. From Figs. 1 (a) and (b), we can observe that the behaviors of A and J_o are mostly the same with increasing electron filling. In the case of Co_2MnSi , both A and J_o of Mn and Co atoms have almost maximum values when the electron number N_e is 29. Meanwhile, in the case of Co_2MnAl , both A and J_o are far away from the maximum values at $N_e = 28$. In addition, it is noted that J_o values at Co sites are smaller than those of Mn sites in both cases. This might indicate that the electronic states of Co sites are more easily affected by the thermal spin fluctuation than those of Mn sites. If we assume that A and J_o at zero temperature determine the Curie temperatures and compare the empirical results, which shows that the Curie temperatures follow an almost linear behavior with respect to the magnetic moments (or number of valence electrons)[58], our results are quite reasonable. We discuss this point deeply in a later section. At this stage, we might conclude that this difference of electron filling contributes to the significant difference in the exchange stiffness constants of Co_2MnSi and Co_2MnAl with $L2_1$ structure at zero temperature.

In addition to the electron filling dependence of A and J_o , we show the density of states (DOS) of Co_2MnSi and Co_2MnAl

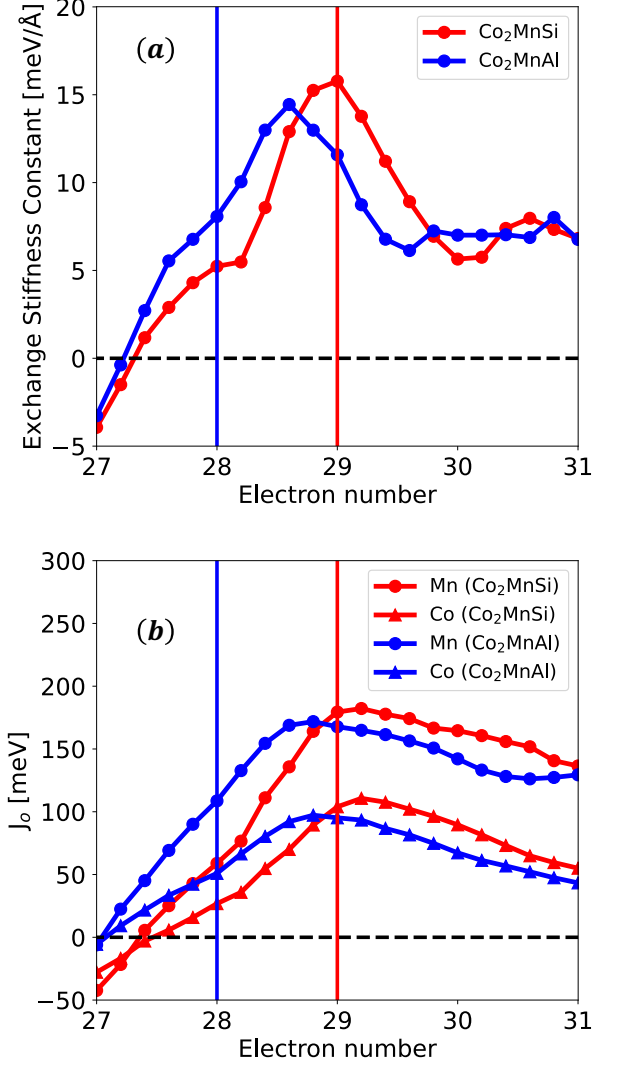
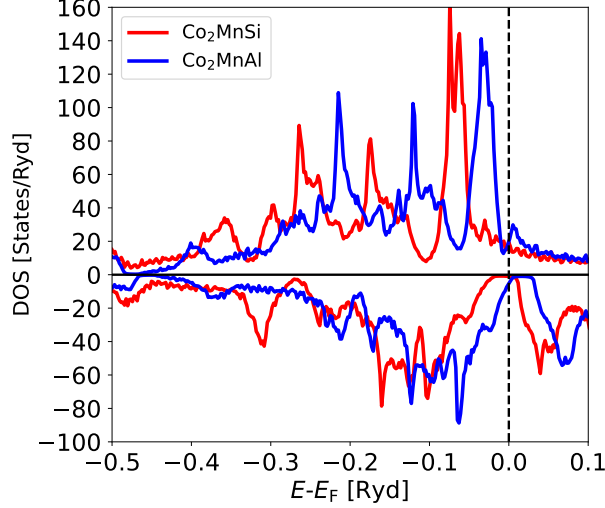


FIG. 1. Electron filling dependence of (a) exchange stiffness constant A and (b) J_o at Mn and Co sites of Co_2MnSi (red lines) and Co_2MnAl (blue lines) with $L2_1$ structure at zero temperature. The vertical lines correspond to the valence electron number of the corresponding alloy.

with $L2_1$ structure in Fig. 2. As we can observe from the figure, the Fermi level of Co_2MnSi is located in the gap in the minority spin state and the half-metallic state is achieved. Further, in the DOS of Co_2MnAl with $L2_1$ structure, the Fermi level is located near the gap in the minority spin state and the half metallicity becomes worse. Judging from Fig. 1 and Fig. 2, we may conclude that, if the Fermi level is located in the gap, A and J_o become large value because the magnetic excitations caused by spin flip are suppressed due to the absence of the minority spin states at zero temperature.

TABLE I. Calculated magnetic properties of Co_2MnSi and Co_2MnAl at zero temperature.

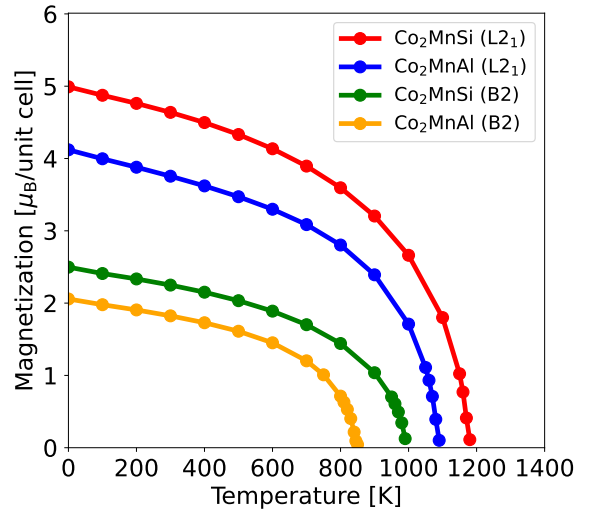
System	A [meV/Å]	D [meV ²]	M_{Co} [μ_B]	M_{Mn} [μ_B]	M_{Total} [μ_B]
Co_2MnSi L_{21}	15.79	571.9	1.090	2.886	4.992
Co_2MnAl L_{21}	8.07	374.4	0.812	2.637	4.120
Co_2MnSi B2	11.98	435.1	1.088	2.890	2.497
Co_2MnAl B2	10.08	467.2	0.785	2.654	2.057

FIG. 2. Density of states of Co_2MnSi (Red) and Co_2MnAl (Blue) with L_{21} structure at zero temperature.

B. Finite-temperature properties

To perform further investigations, we conducted DLM-CPA calculations to examine the finite-temperature magnetic properties of these alloys. We show the calculated temperature dependence of the magnetization of Co_2MnSi and Co_2MnAl in Fig. 3. The calculated Curie temperatures are 1190 and 1090 K for the L_{21} structure of Co_2MnSi and Co_2MnAl and 1000 and 850 K for the B2 structure of Co_2MnSi and Co_2MnAl , respectively. In previous works, the Curie temperatures predicted with the DLM-CPA method were 1103 and 898 K for the L_{21} and B2 structures of Co_2MnSi [55] and 1000 and 800 K for the L_{21} and B2 structures of Co_2MnAl [42], respectively. Our results are close to previously calculated values with the DLM-CPA method. Experimentally, 985[59] and 726 K[60] were reported for Co_2MnSi and Co_2MnAl with L_{21} structures, respectively. The overestimation of the Curie temperature might be attributed to the single-site approximation in the CPA section. An astonishing point of our results is that our calculated Curie temperatures for Co_2MnSi and Co_2MnAl with the L_{21} structure have small differences between them, although their calculated A and J_o values at zero temperature exhibit differences of almost twice between them. Here, let us compare the results of other type of theories. Chico et al.[61] calculated

the Curie temperatures of Co_2MnSi and Co_2MnAl by using the effective Heisenberg Hamiltonian combined with the LAG formula and the Monte Carlo simulation. They reported 750 and 360 K for Co_2MnSi and Co_2MnAl , respectively, using the LSDA and ASA. In addition, they also reported that the calculated spin stiffness constant of Co_2MnAl is nearly half that of Co_2MnSi . This trend is consistent with their predicted Curie temperatures. They also concluded that using the full potential scheme can improve the results. However, an even larger Curie temperature has been predicted using the ASA in our case of Co_2MnAl . Furthermore, Kübler et al.[22, 54] also calculated the Curie temperatures of these alloys with the random phase approximation. Their obtained results are quite in good agreement with experimental results. In their method, they estimated the exchange energy from spin-spiral excitation energy. Judging from our results and their results, mapping to an effective Heisenberg model with the LKAG might underestimate the Curie temperature of Co_2MnAl , reflecting a small spin stiffness constant at zero temperature.

FIG. 3. Temperature dependence of total magnetization per unit cell for Co_2MnSi (Red) and Co_2MnAl (Blue) with L_{21} structures and Co_2MnSi (Green) and Co_2MnAl (Yellow) with B2 structures, respectively.

To examine the origin of the high Curie temperature of Co_2MnAl with the L_{21} structure regardless of the small exchange stiffness constant at zero temperature in our method,

we calculated the temperature dependence of the exchange stiffness constant of Co_2MnSi and Co_2MnAl with L2_1 and B2 structures. The calculated results are shown in Fig. 4. We can see that the calculated temperature dependence of the exchange stiffness constant of Co_2MnSi with the L2_1 structure decrease monotonically with increasing temperatures. Meanwhile, we can also see that the behavior of the exchange stiffness constant of Co_2MnAl with the L2_1 structure is quite different from that of Co_2MnSi . It increases with increasing temperatures up to 200 K, and afterwards it starts to decrease. This means that the exchange stiffness constant is robust against increasing temperatures for Co_2MnAl with the L2_1 structure. If we assume that the temperature dependence of the exchange stiffness constant is the same as that of Co_2MnSi , which is a monotonically decreasing behavior, a lower Curie temperature might be expected for Co_2MnAl and that is consistent with the prediction from exchange interactions at zero temperature. Our results indicate that the Curie temperatures are not simply determined by the exchange interactions at zero temperature. In contrast to the cases of the L2_1 structures, the behaviors of the exchange stiffness constants of the B2 structures at finite temperatures are simple. They decrease monotonically with increasing temperatures. Experimentally, the reported spin (exchange) stiffness constants D (A) for Co_2MnSi are $D = 466 \text{ meV}^2$ [12] and 334 meV^2 [16] from the temperature dependence of magnetization at low temperature. In the Brillouin light scattering spectroscopy experiment at room temperature, 586 meV^2 [14, 15] was reported ($A = 14.67 \text{ meV/Å}$). Meanwhile, for Co_2MnAl , it was reported that $D = 190 \text{ meV}^2$ ($A = 2.996 \text{ meV/Å}$) [15] from the Brillouin light scattering spectroscopy experiment, and $D = 288 \text{ meV}^2$ [16] from the temperature dependence of magnetization at low temperature.

As we have seen above, the difference in the behaviors of temperature dependence of the exchange stiffness constants of the L2_1 structures are unique. To investigate the origin of these behaviors, we calculated the temperature dependence of spin polarization at the chemical potential μ of Co_2MnSi and Co_2MnAl for both structures. The spin polarization ratio P at μ is defined as follows:

$$P(T) = \frac{D^\uparrow(T) - D^\downarrow(T)}{D^\uparrow(T) + D^\downarrow(T)} \times 100, \quad (32)$$

$$D^\sigma(T) = -\frac{1}{\pi} \text{ImTr}_{iL} \int d\mathbf{e}_i \omega_i(\mathbf{e}_i, T) G_{ii}^{\sigma\sigma}(\mu, \mathbf{e}_i), \quad (33)$$

where μ is determined so that the following condition is satisfied:

$$N_e = -\frac{1}{\pi} \text{ImTr}_{iL\sigma} \int_{-\infty}^{\infty} d\epsilon f(\epsilon, T, \mu) \int d\mathbf{e}_i \omega_i(\mathbf{e}_i, T) G_{ii}^{\sigma\sigma}(\epsilon, \mathbf{e}_i). \quad (34)$$

From these figures, we can see that the spin polarization $P(T)$ of Co_2MnSi monotonically decreases with increasing

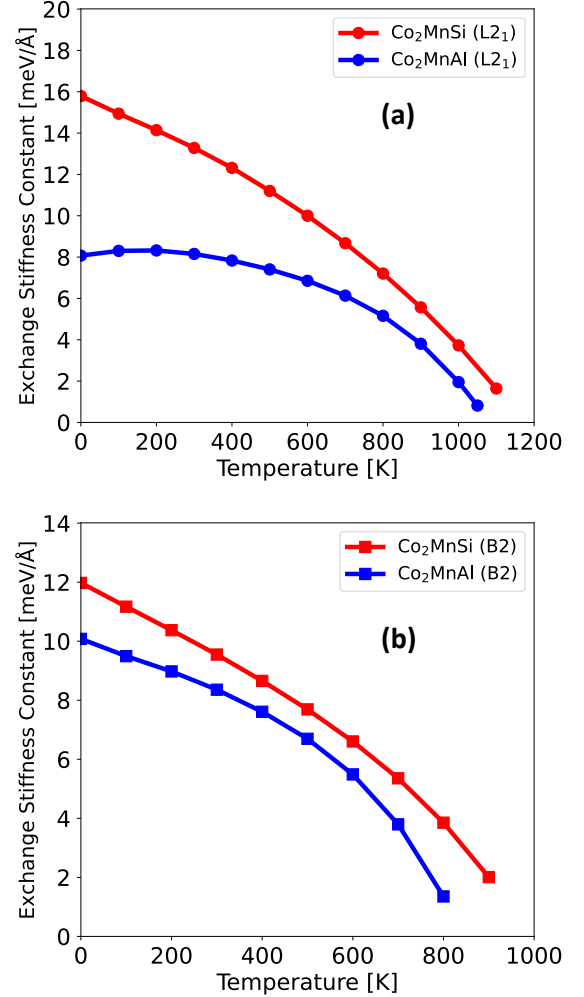


FIG. 4. Calculated temperature dependence of the exchange stiffness constant of Co_2MnSi and Co_2MnAl with (a) L2_1 structure and (b) B2 structure.

temperatures for both structures. These results are consistent with the results calculated by Nawa et al.[55]. This clearly indicates that the half metallicity is broken by the thermal spin fluctuations in Co_2MnSi . Meanwhile, the spin polarization of Co_2MnAl increases with growing temperatures at the low temperature region for the L2_1 structure. This means that the half metallicity is effectively induced due to the spin disorder in Co_2MnAl with the L2_1 structure. In addition, we can see that the temperature dependence of $P(T)$ of Co_2MnAl with the B2 structure is more robust than that of Co_2MnSi . It is worth mentioning the following fact. Oogane et al.[6] experimentally measured the temperature dependence of the TMR ratios for L2_1 Co_2MnSi - and B2 Co_2MnAl -based MTJs. They showed that the temperature dependence of the TMR ratio for the B2 Co_2MnAl -based MTJ is more robust than the MTJ based on the L2_1 Co_2MnSi . These experimental facts may be connected to our temperature dependence of the

spin-polarization ratio of these alloys obtained by the DLM picture.

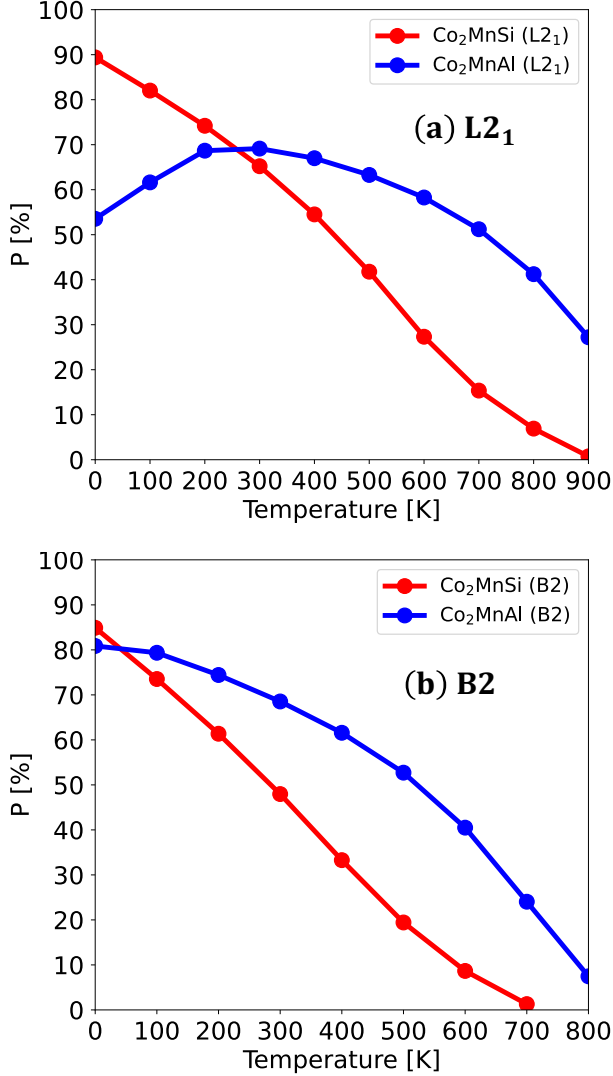


FIG. 5. Temperature dependence of spin polarization at the chemical potential $\mu(T)$ of Co₂MnSi and Co₂MnAl with (a) L₂₁ structure and (b) B2 structure.

Finally, to confirm what we discussed above, we examined the temperature dependence of the density of states of these alloys near the chemical potential, focusing on L₂₁ structures. The calculated results are shown in Fig. 6. From Fig. 6 (a), we can observe that the gap in the minority spin states starts to collapse and the states start to be occupied with increasing temperatures. This means that the half metallicity of Co₂MnSi is monotonically destroyed by the spin disorder due to the thermal spin transverse fluctuations. In the case of Co₂MnAl, shown in Fig. 6 (b), although the gap in the minority spin states itself is destroyed by the spin disorder, the states in the minority spin state become less occupied with in-

creasing temperature in the range up to 400 K. This means that the half metallicity is recovered effectively by the thermal spin transverse fluctuations in Co₂MnAl. This trend is consistent with the behavior of the temperature dependence of the spin polarization ratio discussed above and has been also confirmed by Sakuma et al.[42] for the temperature dependence of the spin-resolved longitudinal conductivity with the Co₂MnAl of L₂₁ structure. Judging from the results in Fig. 1, Fig. 4, and Fig. 6, the spin disorder effect due to thermal spin fluctuations effectively induces half metallicity and it may lead to the change of exchange interactions. Further, this may contribute to the robustness of the exchange stiffness constant at finite temperatures and lead to high Curie temperature, in contrast to the small exchange stiffness constant at zero temperature. In addition, this effect might be connected to the spin configuration dependence of the exchange interactions in metallic magnetic systems, as suggested by several authors.[62–66]. In our case, it could be considered that it is caused by the renormalization of the electronic structure due to the scattering potential of the spin disorders.

However, several points should be improved in this study. Our finite-temperature treatment neglects the longitudinal spin fluctuation. However, the importance of the longitudinal fluctuation for exchange interactions of Co atoms in Co₂FeSi[67] has been recently indicated. We also confirmed that the magnetic moments of Co atoms vanish in the self-consistent DLM calculations, which include only up and down spin states with equal ratio in the CPA section, for both Co₂MnSi and Co₂MnAl with L₂₁ structures. This means that *d* electrons in Co atoms are more itinerant than those in Mn atoms, and their magnetic states might be close to those in fcc Co[68–70]. In addition, it might be considered that the magnetic moments of Co atoms are sustained by the longitudinal spin fluctuations near Curie temperatures or above[21, 30, 71]. Our treatment is based on the force theorem, and the variation in length of magnetic moments is neglected. This might be problematic near Curie temperatures. Therefore, the effect of longitudinal fluctuations for the half metallicity[72] of Co₂MnSi and Co₂MnAl should be investigated in a further study. However, the unique behavior of the electronic structure of Co₂MnAl is found in the low temperature region, and thus, our approximation might not be problematic for these phenomena.

Our treatment is based on static approximations. According to the results with the dynamical mean field theory (DMFT)[73], which can include the dynamical component of spin fluctuations, it has been shown that the non-quasiparticle states described by the local self energy contribute to a reduction in the spin polarization ratio of Co₂MnSi at finite temperatures. This effect on the result of the DOS of Co₂MnAl at finite temperatures could be a target of research from the theoretical view. However, it may be worth mentioning that non-quasiparticle states near Fermi level at finite temperatures and altering the DOS in the majority spin state, both predicted from DMFT calculation results, are not confirmed experimentally in Co₂MnSi[74]. Furthermore, investigating beyond the single-site approximation in the CPA section could also be of interest for further studies.

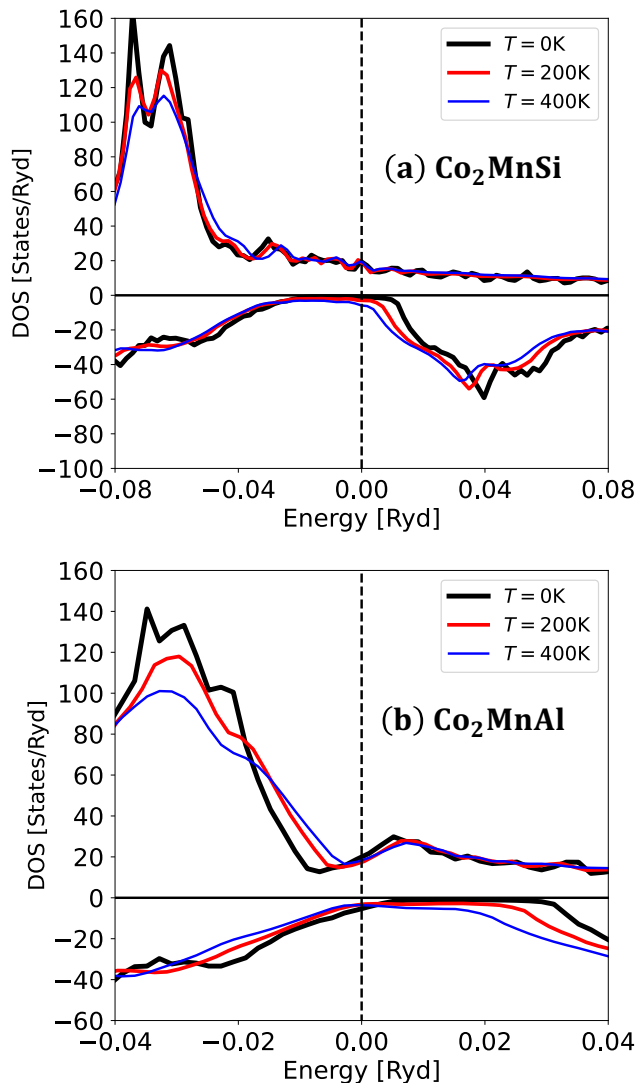


FIG. 6. Temperature dependence of the density of states (DOS) of (a) Co_2MnSi and (b) Co_2MnAl with $L2_1$ structure. The vertical lines correspond to the chemical potential for each temperature.

IV. SUMMARY

In this study, we investigated the magnetic properties, such as exchange stiffness constants, not only at zero temperature but also at finite temperatures, of Co-based full-Heusler alloys, Co_2MnSi and Co_2MnAl , assuming $L2_1$ and B2 structures with the DLM-CPA method. We confirmed the relatively small ex-

change stiffness constant for Co_2MnAl with the $L2_1$ structure at zero temperature compared to that of Co_2MnSi with the $L2_1$ structure. This might be related to the half-metallic electronic structures and the filling dependence of exchange interactions. However, the calculated Curie temperature of Co_2MnAl with the $L2_1$ structure is not very different from that of Co_2MnSi with $L2_1$ structure, contrary to the expectation from the exchange stiffness constant at zero temperature. The behavior of the calculated temperature dependences of the exchange stiffness constant of Co_2MnAl with the $L2_1$ structure is unique compared to that of Co_2MnSi with the $L2_1$ structure. It shows robust behavior against increasing temperatures in the low temperature region. This behavior of the exchange stiffness constant might contribute to determine the high Curie temperature of Co_2MnAl with the $L2_1$ structure. Meanwhile, regarding the results of the B2 structures, the exchange stiffness constants monotonically decrease with increasing temperatures for both alloys.

To investigate the origin of the behavior of the exchange stiffness constant of Co_2MnAl with the $L2_1$ structure at finite temperatures, we examined the temperature dependence of the spin polarization ratio at μ of both alloys. For Co_2MnSi , the gap in the minority spin states is destroyed due to the thermal spin disorder, and it leads to a monotonically decreasing behavior of the spin polarization in both structures. However, in the case of Co_2MnAl with the $L2_1$ structure, although the gap in the minority spin states is also destroyed, the population of electrons in the minority spin states at μ is reduced due to the change of the DOS caused by spin disorder. It might be considered that this leads to the increase in spin polarization at the low temperature region and the robustness of the exchange stiffness constant against increasing temperatures. In addition, the temperature dependence of the spin polarization at μ of Co_2MnAl with the B2 structure is also robust with increasing temperature compared with that of Co_2MnSi .

Our result may indicate that the Curie temperatures of itinerant magnets are not simply determined by the exchange interactions at zero temperature, and the temperature variations of the electronic structure due to spin disorders are also important for the exchange interactions at finite temperatures of the systems.

ACKNOWLEDGMENTS

This work was partly supported by the Center for Science and Innovation in Spintronics (CSIS) and the Center for Innovative Integrated Electronic System (CIES) in Tohoku University and the SIP project, and the X-nics project.

- [1] J. Kübler, A. R. Williams, and C. B. Sommers, Phys. Rev. B **28**, 1745 (1983).
- [2] I. Galanakis, P. H. Dederichs, and N. Papanikolaou, Phys. Rev. B **66**, 174429 (2002).

- [3] I. Galanakis, Ph. Mavropoulos, and P. H. Dederichs, J. Phys. D **39**, 765 (2006).
- [4] Y. Sakuraba, T. Miyakoshi, M. Oogane, Y. Ando, A. Sakuma, T. Miyazaki, and H. Kubota, Appl. Phys. Lett. **89**, 052508 (2006).

- [5] Y. Sakuraba, J. Nakata, M. Oogane, Y. Ando, H. Kato, A. Sakuma, T. Miyazaki, and H. Kubota, *Appl. Phys. Lett.* **89**, 022503 (2006).
- [6] M. Oogane, Y. Sakuraba, J. Nakata, H. Kubota, Y. Ando, A. Sakuma, and T. Miyazaki, *J. Phys. D* **39**, 834 (2006).
- [7] Y. Sakuraba, M. Hattori, M. Oogane, Y. Ando, H. Kato, A. Sakuma, T. Miyazaki, and H. Kubota, *Appl. Phys. Lett.* **88**, 192508 (2006).
- [8] S. Tsunegi, Y. Sakuraba, M. Oogane, K. Takanashi, and Y. Ando, *Appl. Phys. Lett.* **93**, 112506 (2008).
- [9] S. Tsunegi, Y. Sakuraba, M. Oogane, H. Naganuma, K. Takanashi, and Y. Ando, *Appl. Phys. Lett.* **94**, 252503 (2009).
- [10] A. Sakuma, Y. Toga, and H. Tsuchiura, *J. Appl. Phys.* **105**, 07C910 (2009).
- [11] Y. Miura, K. Abe, and M. Shirai, *Phys. Rev. B* **83**, 214411 (2011).
- [12] L. Ritchie, G. Xiao, Y. Ji, T. Y. Chen, C. L. Chien, M. Zhang, J. Chen, Z. Liu, G. Wu, and X. X. Zhang, *Phys. Rev. B* **68**, 104430 (2003).
- [13] B. Rameev, F. Yildiz, S. Kazan, B. Aktas, A. Gupta, L. R. Tagirov, D. Rata, D. Buerger, P. Gruenberg, C. M. Schneider, S. Kämmerer, G. Reiss, and A. Hütten, *Phys. Stat. Soli.* **203**, 1503 (2006).
- [14] J. Hamrle, O. Gaier, S.-G. Min, B. Hillebrands, Y. Sakuraba, and Y. Ando, *J. Phys. D* **42**, 084005 (2009).
- [15] T. Kubota, J. Hamrle, Y. Sakuraba, O. Gaier, M. Oogane, A. Sakuma, B. Hillebrands, K. Takanashi, and Y. Ando, *J. Appl. Phys.* **106**, 113907 (2009).
- [16] R. Umetsu, A. Okubo, A. Fujita, T. Kanomata, K. Ishida, and R. Kainuma, *IEEE Trans. Magn.* **47**, 2451 (2011).
- [17] F. J. Dyson, *Phys. Rev.* **102**, 1217 (1956).
- [18] N. D. Telling, P. S. Keatley, G. van der Laan, R. J. Hicken, E. Arenholz, Y. Sakuraba, M. Oogane, Y. Ando, and T. Miyazaki, *Phys. Rev. B* **74**, 224439 (2006).
- [19] N. D. Telling, P. S. Keatley, G. van der Laan, R. J. Hicken, E. Arenholz, Y. Sakuraba, M. Oogane, Y. Ando, K. Takanashi, A. Sakuma, and T. Miyazaki, *Phys. Rev. B* **78**, 184438 (2008).
- [20] G. H. Fecher, D. Ebke, S. Ouardi, S. Agrestini, C. Y. Kuo, N. Hollmann, Z. Hu, A. Gloskovskii, F. Yakhov, N. B. Brookes, and C. Felser, *SPIN* **04**, 1440017 (2014).
- [21] T. Moriya, *Spin Fluctuations in Itinerant Electron Magnetism* (Springer, Berlin, 1985).
- [22] J. Kübler, *Theory of Itinerant Electron Magnetism* (Oxford University Press, New York, 2009).
- [23] A. Sakuma, *J. Phys. Soc. Jpn.* **93**, 054705 (2024).
- [24] S. Yamashita and A. Sakuma, *J. Appl. Phys.* **136**, 013903 (2024).
- [25] M. Cyrot, *Phys. Rev. Lett.* **25**, 871 (1970).
- [26] J. Hubbard, *Phys. Rev. B* **19**, 2626 (1979).
- [27] J. Hubbard, *Phys. Rev. B* **20**, 4584 (1979).
- [28] H. Hasegawa, *J. Phys. Soc. Jpn.* **46**, 1504 (1979).
- [29] H. Hasegawa, *J. Phys. Soc. Jpn.* **49**, 178 (1980).
- [30] H. Hasegawa, *J. Phys. Soc. Jpn.* **49**, 963 (1980).
- [31] T. Oguchi, K. Terakura, and N. Hamada, *J. Phys. F* **13**, 145 (1983).
- [32] A. J. Pindor, J. Staunton, G. M. Stocks, and H. Winter, *J. Phys. F* **13**, 979 (1983).
- [33] J. Staunton, B. L. Gyorffy, A. J. Pindor, G. M. Stocks, and H. Winter, *J. Magn. Magn. Mater.* **45**, 15 (1984).
- [34] B. L. Gyorffy, A. J. Pindor, J. Staunton, G. M. Stocks, and H. Winter, *J. Phys. F* **15**, 1337 (1985).
- [35] J. B. Staunton and B. L. Gyorffy, *Phys. Rev. Lett.* **69**, 371 (1992).
- [36] J. B. Staunton, S. Ostanin, S. S. A. Razee, B. L. Gyorffy, L. Szunyogh, B. Ginatempo, and E. Bruno, *Phys. Rev. Lett.* **93**, 257204 (2004).
- [37] J. B. Staunton, L. Szunyogh, A. Buruzs, B. L. Gyorffy, S. Ostanin, and L. Udvardi, *Phys. Rev. B* **74**, 144411 (2006).
- [38] S. Yamashita and A. Sakuma, *J. Phys. Soc. Jpn.* **91**, 093703 (2022).
- [39] S. Yamashita and A. Sakuma, *Phys. Rev. B* **108**, 054411 (2023).
- [40] R. Hiramatsu, D. Miura, and A. Sakuma, *Appl. Phys. Express* **15**, 013003 (2021).
- [41] R. Hiramatsu, D. Miura, and A. Sakuma, *J. Phys. Soc. Jpn.* **92**, 044704 (2023).
- [42] A. Sakuma and D. Miura, *J. Phys. Soc. Jpn.* **91**, 084701 (2022).
- [43] A. Sakuma, *J. Phys. Soc. Jpn.* **69**, 3072 (2000).
- [44] O. K. Andersen, Z. Pawłowska, and O. Jepsen, *Phys. Rev. B*, **34**, 5253 (1986).
- [45] I. Turek, V. Drchal, J. Kudrnovský, M. Šöb, and P. Weinberger, *Electronic Structure of Disordered Alloys, Surfaces and Interfaces* (Kluwer Academic, Dordrecht, 1997).
- [46] J. Kudrnovský and V. Drchal, *Phys. Rev. B*, **41**, 7515 (1990).
- [47] H. L. Skriver, *The LMTO Method* (Springer, Berlin, 1984).
- [48] L. M. Sandratskii, *Phys. Status Solidi B* **136**, 167 (1986).
- [49] O. N. Mryasov, V. A. Gubanov, and A. I. Liechtenstein, *Phys. Rev. B* **45**, 12330 (1992).
- [50] M. Uhl, L. Sandratskii, and J. Kübler, *J. Magn. Magn. Mater.* **103**, 314 (1992).
- [51] J. Kübler, *J. Phys.: Condens. Matter* **18**, 9795 (2006).
- [52] S. Yamashita and A. Sakuma, *Appl. Phys. Express* **16**, 083002 (2023).
- [53] S. Yamashita and A. Sakuma, *Jpn. J. Appl. Phys.* **63**, 025501 (2024).
- [54] J. Kübler, G. H. Fecher, and C. Felser, *Phys. Rev. B* **76**, 024414 (2007).
- [55] K. Nawa, I. Kurniawan, K. Masuda, Y. Miura, C. E. Patrick, and J. B. Staunton, *Phys. Rev. B* **102**, 054424 (2020).
- [56] A. I. Liechtenstein, M. I. Katsnelson, V. P. Antropov, and V. A. Gubanov, *J. Magn. Magn. Mater.* **67**, 65 (1987).
- [57] A. Sakuma, *J. Phys. Soc. Jpn.* **68**, 620 (1999).
- [58] G. H. Fecher, H. C. Kandpal, S. Wurmehl, C. Felser, and Gerd Schönhense, *J. Appl. Phys.* **99**, 08J106 (2006).
- [59] K. H. J. Buschow, P. G. van Engen, and R. Jongebreur, *J. Magn. Magn. Mater.* **38**, 1 (1983).
- [60] R. Y. Umetsu, K. Kobayashi, A. Fujita, R. Kainuma, and K. Ishida, *J. Phys. Appl. Phys.* **103**, 07D718 (2008).
- [61] J. Chico, S. Keshavarz, Y. Kvashnin, M. Prereiro, I. D. Marco, C. Etz, O. Eriksson, A. Bergman, and L. Bergqvist, *Phys. Rev. B* **93**, 214439 (2016).
- [62] L. M. Small and V. Heine, *J. Phys. F: Met. Phys.* **14**, 3041 (1984).
- [63] V. Heine, A. I. Liechtenstein, and O. N. Mryasov, *Europhys. Lett.* **12**, 545 (1990).
- [64] M. U. Luchini and V. Heine, *Europhys. Lett.* **14**, 609 (1991).
- [65] O. N. Mryasov, A. J. Freeman, and A. I. Liechtenstein, *J. Appl. Phys.* **79**, 4805 (1996).
- [66] S. Khmelevskiy, T. Khmelevska, A. V. Ruban, and P. Mohn, *J. Phys.: Condens. Matter* **19**, 326218 (2007).
- [67] S. Khmelevskiy and P. Mohn, *J. Magn. Magn. Mater.* **560**, 169615 (2022).
- [68] M. Uhl and J. Kübler, *Phys. Rev. Lett.* **77**, 334 (1996).
- [69] N. M. Rosengaard and B. Johansson, *Phys. Rev. B* **55**, 14975 (1997).
- [70] S. V. Halilov, H. Eschrig, A. Y. Perlov, and P. M. Oppeneier, *Phys. Rev. B* **58**, 293 (1998).
- [71] V. Heine, J. H. Samson, and C. M. M. Nex, *J. Phys. F: Met. Phys.* **11**, 2645 (1981).
- [72] L. M. Sandratskii, *Phys. Rev. B* **78**, 094425 (2008).
- [73] L. Chioncel, Y. Sakuraba, E. Arrigoni, M. I. Katsnelson, M. Oogane, Y. Ando, T. Miyazaki, E. Burzo, and A. I. Liechtenstein,

Phys. Rev. Lett. **100**, 086402 (2008).

[74] K. Miyamoto, A. Kimura, Y. Miura, M. Shirai, M. Ye, Y. Cui, K. Shimada, H. Namatame, M. Taniguchi, Y. Takeda, Y. Saitoh, E. Ikenaga, S. Ueda, K. Kobayashi, and T. Kanomata, Phys. Rev. B **79**, 100405(R) (2009).